INTERNATIONAL JOURNAL FOR NUMERICAL METHODS IN FLUIDS, VOL. 9, 1073–1086 (1989)

ASSESSMENT OF VARIANTS OF THE k–ε TURBULENCE MODEL FOR ENGINE FLOW APPLICATIONS

B. AHMADI-BEFRUI

Fluid Dynamics Research Department, AVL GmbH, Graz, Austria

AND

A. D. GOSMAN

Fluids Section, Mechanical Engineering Department, Imperial College, London SW7 2BX, U.K.

SUMMARY

This paper is concerned with simulation of the mean flow and turbulence evolution in a model engine and comparison of the behaviour of certain important turbulence parameters, namely the intensity, length scale and dissipation time scale, as predicted by three variants of the k–ε model developed for application to strongly compressible flows. The predictions pertain to the axisymmetric, disc-chamber, four-stroke, Imperial College model engine operating at 200 rpm and compression ratios of 3·5 and 6·7. The paper analyses the predicted variations of these parameters during the induction, compression and expansion strokes and identifies the versions that produce the most consistent and physically plausible variations. The significance, to the turbulence evolution, of the ratio of the turbulence dissipation time scale to the time scale of compression/expansion is also discussed. It is concluded that on these grounds the Morel–Mansour and El Tahry versions are, and the Watkins version is not, suitable for engine applications.

KEY WORDS k–ε turbulence model Compressible flow Bulk dilatation Reciprocating engine flow

INTRODUCTION

The k–ε model is currently used by nearly all researchers developing or applying multi-dimensional methods for prediction of flow and combustion in engines. However, there exist various formulations of the model, in particular of the ε-transport equation, with the differences in all instances residing in the term(s) associated with compressibility effects.[1–5] The purpose of the present study was to determine which, if any, of the proposed versions correctly predicts the turbulence evolution in engines.

The earliest attempt at deriving a suitable formulation of the k–ε model for strongly compressible engine flows was that of Watkins,[1] who revealed the existence in the ε-transport equation of an additional dilatation term of the form $\rho\varepsilon\nabla\cdot\mathbf{U}$. Subsequently Reynolds[6] showed that the coefficient of this term could be determined through the application of rapid distortion theory, and since then the issue has received considerable attention, as evidenced by the development of alternative forms by Morel and Mansour,[2] El Thary[3] and, most recently, by Wu *et al.*[7]

0271–2091/89/091073–14$07.00

Received January 1988
Revised September 1988

Morel and Mansour[2] (hereafter denoted by MM) and El Tahry[3] compared the performances of their proposed ε-transport equations with that of Watkins[1] (in the case of MM, also with the version employed by Ramos and Sirigano,[4] in which the dilatation term is simply neglected), through application to the idealized case of compression and expansion of a homogeneous turbulent field, and revealed substantial differences in the predictions. In particular, these studies indicated that implausible variations of the length scale l are predicted by the Watkins[1] model. However, these studies were not conclusive since they were performed for circumstances leading to the augmentation of turbulence intensity u' during compression, which is contrary to the predicted and measured trends observed for axisymmetric disc-chamber engines.[8,9] This is believed to be due to the fact that because in the aforementioned assessments the induction process was not simulated, arbitrary and, especially in respect of the dissipation time scale τ, non-representative initial conditions were employed.[10] Further, the studies only used the length scale variations during compression and expansion as the criterion for the comparison, whereas there are other significant parameters which also bear examination, notably the turbulence intensity and dissipation time scale as just implied.

Subsequently Ahmadi-Befrui *et al.*[9] attempted an assessment of the aforementioned variants through simulation of the complete engine cycle in the axisymmetric, disc-chamber, four-stroke, Imperial College model engine operating at 200 rpm and compression ratios of 3·5 and 6·7, and comparison with measurements of the ensemble-mean velocity and turbulence intensity. This study showed that for the conditions investigated, the three versions produced closely similar predictions of these quantities in good qualitative and moderate quantitative agreement with the experimental data. Because none of the models produced consistently superior agreement, it was concluded that on the basis of this evidence alone no choice could be made between them.

In a recent study Wu *et al.*[7] applied the Watkins[1] and Reynolds[6] models to the cases of one-dimensional and isotropic compression, at a constant rate of strain S, of unconfined homogeneous turbulence and assessed their performance through comparison of the predicted turbulence energy k and length scale l variations with direct numerical solutions of the Navier–Stokes equations. It was found that the ratio of the turbulence dissipation time scale τ to the imposed strain time scale S^{-1} had significant bearing both on the turbulence behaviour and the performance of the models. The Reynolds[6] model gave superior agreement for 'slow' compression rates (i.e. $\tau S \lesssim 0{\cdot}5$), but both models failed to predict the turbulence behaviour under 'rapid' compression ($\tau S > 2{\cdot}5$) due to incorrect levels of τ being produced by the k–ε model equations. Consequently they proposed a three-equation k–ε–τ turbulence model which produced better overall agreement. It should however be noted that only the low end of the τS range they examined is relevant to the conditions at the start of the compression process in engines, for which τS (S in this instance is the average compression strain rate) is of order 10^{-1};[10] this is true at all engine speeds, since τ is nearly inversely proportional to speed.[10]

This paper complements the previous assessment by the authors[9] and is concerned with a comparison of the predicted variations of the turbulence intensity, length scale and dissipation time scale during the induction, compression and expansion strokes produced by the Watkins, MM and El Tahry models. The results are judged by examining their compatibility and physical plausibility, and comparing with the experimental trends where possible.

THE PREDICTION METHOD

The overall modelling approach used here has been described in several publications (e.g. References 9 and 11). The flow is represented by the density-weighted ensemble-averaged (DWEA) differential conservation equations of mass, momentum and stagnation enthalpy, in

addition to the transport equations for the turbulence energy k and its dissipation rate ε. The correlations of the fluctuating components appearing in the DWEA equations are modelled, following Bilger[12] and Jones,[13] similar to their counterparts in constant density flows. The modelled forms are, in Cartesian tensor notation,

$$\frac{\partial \rho}{\partial t} + \frac{\partial}{\partial x_j}(\rho U_j) = 0, \tag{1}$$

$$\frac{\partial}{\partial t}(\rho U_i) + \frac{\partial}{\partial x_j}(\rho U_j U_i) = -\frac{\partial P}{\partial x_i} + \frac{\partial}{\partial x_j}(2\mu_T S_{ij}) - \frac{2}{3}\frac{\partial}{\partial x_i}(\mu_T D + \rho k), \tag{2}$$

$$\frac{\partial}{\partial t}(\rho h) + \frac{\partial}{\partial x_j}(\rho U_j h) = \frac{\partial P}{\partial t} + \frac{\partial}{\partial x_j}\left(\frac{\mu_T}{\sigma_h}\frac{\partial h}{\partial x_j}\right), \tag{3}$$

where ρ is the density, P is the pressure, h is the stagnation enthalpy, σ_h is the turbulence Prandtl number, U_i and x_i are respectively the i-direction velocity and co-ordinate direction, S_{ij} is the strain rate tensor given by

$$S_{ij} = \frac{1}{2}\left(\frac{\partial U_i}{\partial x_j} + \frac{\partial U_j}{\partial x_i}\right), \tag{4}$$

and D is the velocity divergence:

$$D = S_{ii} \equiv \nabla \cdot \mathbf{U} \quad \left(= -\frac{1}{\rho}\frac{\partial \rho}{\partial t} \text{ for } \frac{\partial \rho}{\partial x_j} = 0\right). \tag{5}$$

The turbulent viscosity μ_T in the above is defined as

$$\mu_T = C_\mu \rho k^2/\varepsilon, \tag{6}$$

where C_μ is an empirical constant ($C_\mu = 0{\cdot}09$), k is the DWEA turbulence energy and ε is its dissipation rate.

The transport equation for k, which as already noted has the same form for all models considered, is

$$\frac{\partial}{\partial t}(\rho k) + \frac{\partial}{\partial x_j}(\rho U_j k) = \frac{\partial}{\partial x_j}\left(\frac{\mu_T}{\sigma_k}\frac{\partial k}{\partial x_j}\right) + 2\mu_T S_{ij} S_{ij} - \tfrac{2}{3}(\mu_T D^2 + \rho k D) - \rho\varepsilon. \tag{7}$$

The different versions of the ε-transport equation may be collectively represented by

$$\frac{\partial}{\partial t}(\rho\varepsilon) + \frac{\partial}{\partial x_j}(\rho\varepsilon U_j) = \frac{\partial}{\partial x_j}\left(\frac{\mu_T}{\sigma_\varepsilon}\frac{\partial \varepsilon}{\partial x_j}\right) + \frac{\varepsilon}{k}[2C_1 \mu_T S_{ij} S_{ij} - \tfrac{2}{3}(C_1' \mu_T D^2 + C_1'' \rho k D)]$$
$$+ C_3 \rho\varepsilon D + C_4 \frac{\rho\varepsilon}{\mu}\frac{\partial \mu}{\partial t} - C_2 \frac{\rho\varepsilon^2}{k}, \tag{8}$$

where the coefficients C_1', C_1'', etc. differ according to the version, as indicated in Table I.

Watkins[1] arrived at his version by deriving the k–ε set for a general compressible flow, according to Harlow and Nakayama's[14] approach, in a semi-rigorous fashion, without specific reference to engine circumstances; in particular, turbulent fluctuations of density were ignored.

Reynolds[6] adopted a different approach in which he required the model to produce the correct behaviour for the limiting case of rapid spherical compression of a homogeneous turbulent field. This analysis resulted in a single compressibility term of the form.

$$C_3 \rho\varepsilon \nabla \cdot \mathbf{U},$$

Table I. Values of coefficients appearing in the ε-transport equation (8) according to different investigators

Investigator	C_1	C_1'	C_1''	C_2	C_3	C_4
Watkins[1]	1·44	1·44	1·44	1·92	1	0
Reynolds[6]*	1·44	1·44	1·44	1·92	−0·373	0
Moreland Mansour[2]	1·44	1·32–1·44	3·5–4·5	1·92	1	0
El Tahry[3]	1·44	1·44	1·44	1·92	−1/3	1

* The coefficient values for this entry have been adjusted slightly to bring the C_1 and C_2 coefficients into line with those for other investigators, so as to facilitate comparison of the coefficients relating to compressibility.

with

$$C_3 = \tfrac{2}{3}(2 - C_1).$$

Morel and Mansour[2] generalized Reynolds' analysis to the case of a general compressing strain field, requiring that the eddy length scale vary in accord with the volume change of the flow field. This analysis, for $C_3 = 1$ (the accepted value), rendered C_1' and C_1'' functions of the strain field. Table I shows the range of values implied by these functions, which are employed in their full forms in the present study and are quoted in Appendix I.

El Tahry[3] followed the approach of Harlow and Nakayama[14] but also modelled the correlations involving density fluctuations. This resulted in a value of $C_3 = -1/3$ and an additional compressibility term* of the form

$$C_4 \frac{\rho\varepsilon}{\mu}\frac{\partial \mu}{\partial t},$$

where μ is the molecular viscosity. This term can be recast as

$$C_4 \rho\varepsilon \nabla \cdot \mathbf{U}$$

by expressing μ as a function of temperature and assuming a polytropic compression/expansion, as shown in Appendix II. The coefficient C_4 then lies in the range $-0{\cdot}15$ to $-0{\cdot}25$, for the range of temperature variations typical of the engine compression/expansion processes. Therefore the C_3 and C_4 terms may be physically interpreted as representing the influence of bulk dilatation on the dissipation rate respectively via its direct effect on the turbulence length scale (the large scale) and through variations in the molecular viscosity caused by the bulk temperature variations (affecting the dissipation scales).

The RPM numerical procedure used to solve the foregoing equations and the treatment of the boundary conditions are outlined in Reference 9 and given in more detail in References 10 and 11. The inlet/exhaust boundary conditions are deduced from the calculated instantaneous mass flow rate and prescribed at the valve exit plane, with the aid of the experimental data, according to the practice described in Reference 9. At solid surfaces the appropriate conditions are imposed via 'wall-functions', based upon the assumption of logarithmic velocity and temperature distributions.

* Additional terms that are of importance only in the presence of combustion (i.e. strong temperature gradients) were also obtained.

PRELIMINARY EXAMINATION OF THE TURBULENCE MODELS

The capability of the models considered to simulate at least qualitatively the effect of bulk dilatation on turbulence can be assessed by examining their degenerate forms for the case of a general unidirectional compression/expansion process acting on a homogeneous turbulence field. For these conditions, equations (7) and (8) reduce to[2,10]

$$\frac{dk}{dt} = \frac{2}{3} a C_\mu \frac{k^2}{\varepsilon} D^2 - \frac{2}{3} kD - \varepsilon, \tag{9}$$

$$\frac{d\varepsilon}{dt} = \frac{\varepsilon}{k}\left(\frac{2}{3}[C_1(1+a) - C_1'] C_\mu \frac{k^2}{\varepsilon} D^2 - \frac{2}{3} C_1'' kD - C_2\varepsilon\right) + C_3 \varepsilon D + C_4 \frac{\varepsilon}{\mu}\frac{\partial \mu}{\partial t}. \tag{10}$$

Here the value of the positive constant 'a' depends on the type of compression (axial, radial or spherical);[2] the following analysis applies to all types.

The k-equation shows that for a compression process ($D < 0$) the 'production' term due to the compressibility effect ($-\frac{2}{3}$kD) is positive and tends to augment turbulence, while for the expansion process ($D > 0$) the reverse holds. This is in accord with the experimental evidence regarding the effect of bulk 'rapid' compression/expansion on turbulence.[15,16] Indeed the computational study of Wu *et al.*[7] shows that, contrary to the arguments put forward by Bradshaw,[17] the present formulation of the turbulence generation term is capable of producing the correct turbulence level for a wide range of compression time scales. Wu *et al.*[7] identify the ε-transport equation as the source of error.

The noteworthy points of the ε-equation (10) for the present circumstances are:

(i) The 'production' and 'destruction' terms are multiplied by the inverse of the dissipation time scale $\tau = (k/\varepsilon)$, while the additional compressibility terms are independent of τ: it follows, therefore, that the relative importance of the compressibility terms depends on the level of τ.

(ii) For the effect of compressibility on ε to be compatible with that on k, then $C_3 - \frac{2}{3} C_1''$ must be negative, i.e. $C_3 < \frac{2}{3} C_1''$.

(iii) For ε to respond correctly to the variations of molecular viscosity, it is necessary that $C_4 > 0$.

It is evident from Table I that the Watkins[1] model does not satisfy condition (ii), i.e. the net effect of the compressibility terms is to tend to reduce ε during compression and increase it during expansion.

RESULTS AND DISCUSSION

The two test cases examined here involve simulation of flow in the four-stroke, disc-chamber, central-valve, Imperial College model engine motored at 200 rpm and having compression ratios of 3·5 (case I) and 6·7 (case II). The calculations were performed on a two-dimensional axisymmetric 45 × 45 computational mesh with a computational time step equivalent to 3° CA. The numerical accuracy of the solutions was assessed and extensively reported in Reference 9 and is sufficient to allow evaluation of the relative merits of the turbulence models under investigation.

The flow evolution

An overall impression of the in-cylinder flow evolution, as represented by the results obtained for case II using the MM turbulence model, is provided in Figure 1 in terms of plots at selected crank angles of the velocity field and the following normalized turbulence parameters:

intensity $u^* = \sqrt{(\frac{2}{3}k)}/V_p$
length scale $l^* = l/B = (C_\mu^{3/4} k^{3/2}/\varepsilon)/B$
time scale $\tau^* = \tau/T_{cycle} = (k/\varepsilon)/T_{cycle}$.

Here V_p, B and T_{cycle} are respectively the mean piston speed, cylinder bore and cycle period (= 60/engine speed). These scales, it should be noted, are not identical to those usually measured

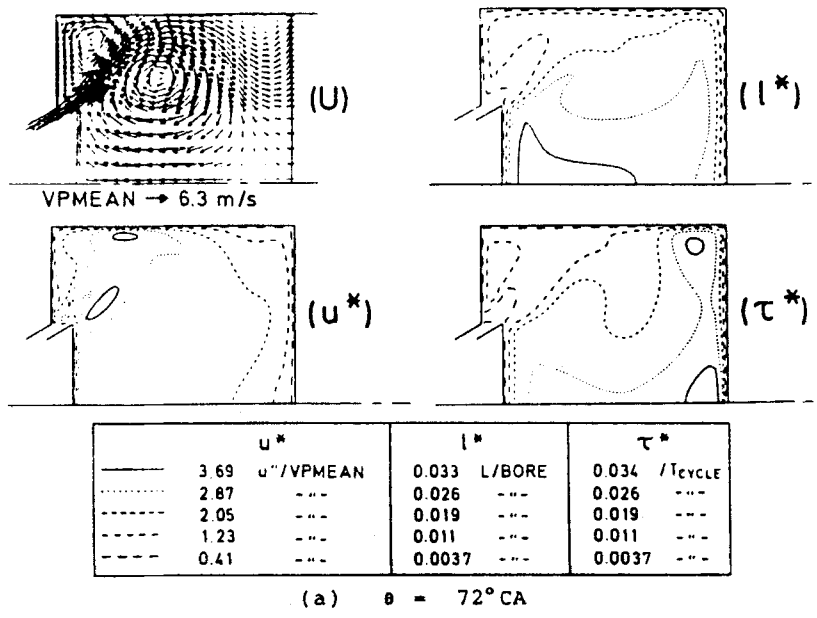

(a) θ = 72° CA

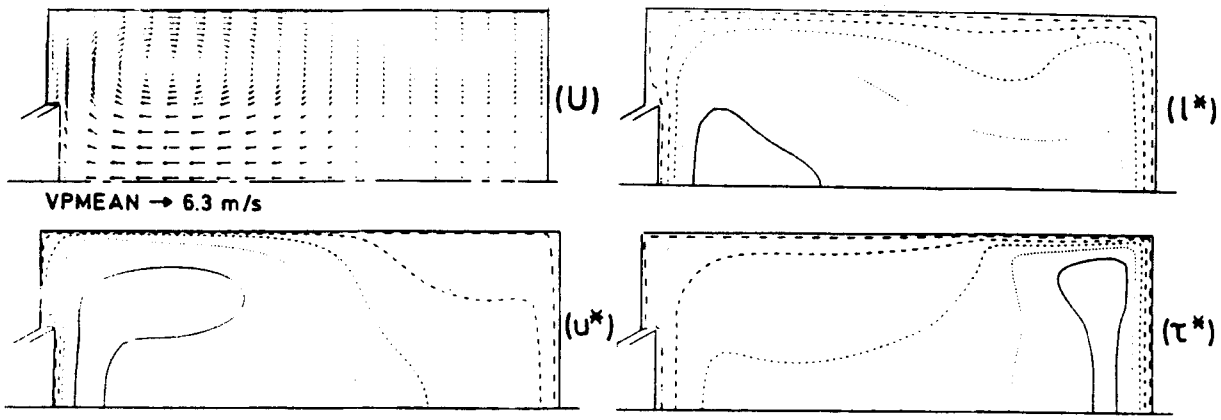

(b) θ = 180° CA

Figure 1. (a, b)

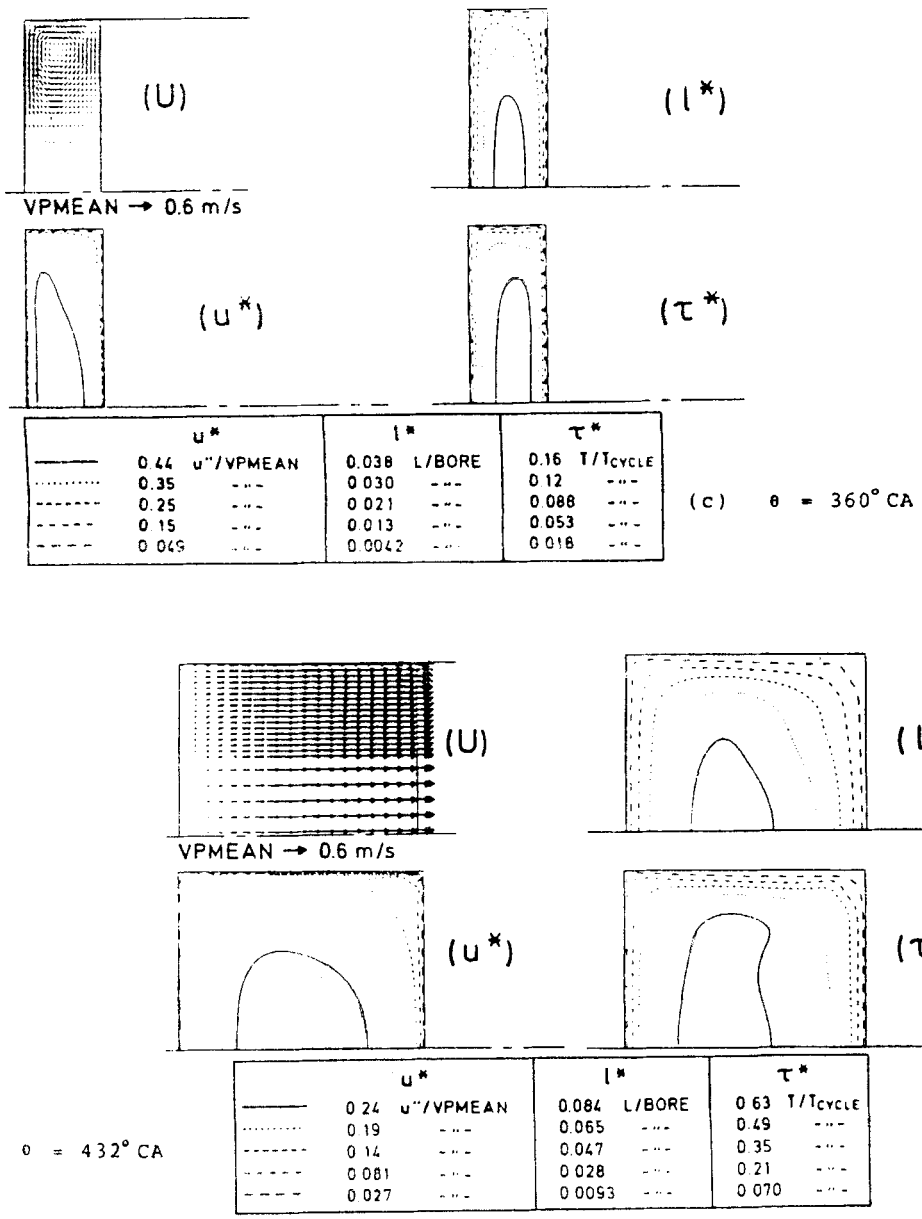

Figure 1. Predictions of velocity field and normalized turbulence parameters u^*, l^* and τ^* at selected crank angles for case II

but bear some relation to them: thus l is of the order of the integral length scale L, and $\tau = \lambda^2/10\nu$, where λ and ν are respectively the Taylor microscale and kinematic viscosity. For equilibrium shear flows, l is identical to the Prandtl mixing length and

$$\tau = \frac{\sqrt{2}}{2} C_\mu^{-1/2} S^{-1},$$

i.e. it is proportional to the time scale of the strain field.[10] The characteristics of the flow evolution are analysed in depth elsewhere[10] and here only a summary is presented.

During early induction (Figure 1(a)) the intake jet separates at the valve seat and head and produces a system of vortices near the cylinder head/wall junction and in the valve wake. The in-cylinder turbulence is predominantly determined by the characteristics of the turbulence generated within the shear layers of this jet. The length scale l^* within the jet is of the order of the valve lift, and outside it is controlled by the engine geometry. The distribution of τ^* shows small levels of the order of $0{\cdot}01\,T_{\text{cycle}}$ ($\simeq 4°$ CA) in the initial region of the jet, increasing rapidly along its path and into the recirculation region, indicating that the jet is the source of the turbulence. These observations and other detailed features reveal that the jet turbulence is in a quasi-steady state of near local-equilibrium.

During the latter part of the induction stroke, the intake jet velocity and turbulence level fall and a well defined turbulence structure evolves within the main vortex in the valve wake. The results at the end of induction (Figure 1(b)) show the disappearance of the structure associated with the intake jet, confirming its quasi-steady equilibrium character, with largest level of u^* now occurring in the main vortex. The length scale is now strongly controlled by the engine geometry, and indeed the maximum levels near the cylinder axis ($l^* = 0{\cdot}07$) are closely similar to those given by the Prandtl mixing length theory for the centre of a fully developed pipe flow.[18] The level of τ^* in the region of the main vortex is $\simeq 0{\cdot}06$, giving $\tau \simeq 22°$ CA.

Throughout compression, the intake-generated vortices weaken and break up, and the turbulence decays and relaxes to a structure predominantly controlled by the engine geometry, as illustrated by Figure 1(c) pertaining to TDC compression.

During expansion, the still persisting main vortex breaks up and the flow becomes predominantly one-dimensional in the direction of piston motion. Turbulence decays rapidly, due to the effect of bulk expansion,[16, 17] and retains its geometry-controlled structure: these features are evident in Figure 1(d).

Predictions of the turbulence model variants

The predicted temporal variations of the normalized quantities $U^* = U/V_p$, u^*, l^* and τ^* produced by the three k–ε variants at the monitoring location $z/B = 0{\cdot}2$ and $r/B = 0{\cdot}33$, where z and r are axial and radial co-ordinates respectively, measured from the centre of the cylinder head, are presented in Figure 2: these pertain to case I. Figure 3 contains similar plots at the location $z/B = 0{\cdot}13$, $r/B = 0{\cdot}33$ for the conditions of case II.*

The results for U^* and u^* in both figures show that during induction the monitoring locations are within the intake jet path: l^* and τ^* show nearly constant levels at this stage, associated with the intake jet turbulence, in accord with experimental data.[19, 20] All models produce identical results during this phase owing to the negligible compressibility effects prevailing at the low engine speed of 200 rpm.

Near the end of induction ($\theta = 150°$–$180°$ CA), the decays of the intake jet velocity and turbulence intensity are accompanied by an apparent increase in l^* and τ^*. Similar rapid changes of turbulence parameters at this stage are evident in the measurements of References 19 and 20, among others, and are attributed mainly to the turbulence decay process.[21] The predictions, however, reveal that these changes are not just a consequence of turbulence decay, but also due to

* In this case the results for $z/B = 0{\cdot}2$ are not directly comparable with those of case I, since they were influenced by wall effects caused by piston proximity near the TDC compression.

the fact that the intake jet structure disappears and the monitoring location is engulfed by the turbulence associated with the main vortex.

The predictions of all models for early compression (θ = 180°–220° CA) are also similar and show that initially the decay of turbulence is accompanied by growth of l^* and τ^*, in accord with the characteristics of the decay of grid-generated turbulence.[22] However, the rate of increase of l^* gradually falls and it tends towards an asymptotic value of l^* = 0·06–0·07. This asymptotic limit observed here is due to the controlling influence of engine geometry on length scale, evident in Figure 1, and is in accord with the experimental findings of Prudnikov[23] concerning the decay of grid-generated turbulence in steady pipe flows.

The results of Figures 2 and 3 show that all variants predict continuous decay of u^* at closely similar rates during the interval θ = 225°–495° CA (although the Watkins[1] version produces a slightly smaller decay rate than the others during the period θ = 270°–330° CA, and larger rates throughout the rest of compression and the expansion stroke). This general behaviour is in agreement with the simulations of Wu *et al.*[7] which exhibited continuous decay of turbulence energy for conditions like those examined here, where τ is small compared to the compression time scale (typically for $\tau^* < 0{\cdot}25$): this is due to the small rate of compression production compared with the dissipation rate of the turbulence energy. The variations of other turbulence parameters produced by different versions are not however all the same, as will now be discussed.

Watkins' version[1] predicts large increases of l^* and τ^* during the interval θ = 225°–330° CA, followed by rapid falls during θ = 330°–495° CA. The increases in l^* and τ^* are in accord with the general characteristics of turbulence decay[22] and in closed vessels[24] and may be justified on the grounds that the decay process overwhelms the effects of compression on turbulence, as was found in Reference 7 for the case of unconfined homogeneous turbulence under slow compression. However, this implies that l is not constrained by the cylinder bore (the predictions imply that the geometric constraint on l is the cylinder head–piston distance throughout the compression stroke). Furthermore, the predicted reductions of l^* and τ^* during the expansion stroke are incompatible with the decay of turbulence intensity and the expected increase of turbulence length scale under dilatation.[25] Also, the increase of l^* near TDC with an increase in compression ratio, evident in Figure 2(c) and 3(c), is physically implausible. The differences between the l^* and τ^* variations produced by this model and the other versions are a consequence of its treatment of the compressibility effect in the ε-equation.

As already noted the MM[2] and El Tahry[3] models produce similar trends to each other for all turbulence parameters during compression and expansion. According to these versions, during compression l^* begins to decrease when the combined influence of compression and the geometric constraint (initially the bore diameter and latterly the cylinder head–piston distance) exceeds that of the decay process, although τ^* increases in accord with the turbulence decay. A noteworthy point is the small reduction of τ^* near TDC for the higher compression-ratio conditions of case II, which is a consequence of augmentation of the turbulence production/dissipation rate due to larger compressibility effects (the dilatation term $\nabla \cdot \mathbf{U}$ and the instantaneous time scale ratio $\tau\, \nabla \cdot \mathbf{U}$ attain maximum levels at θ = 330°–340° CA). The behaviour of τ^* is in agreement with experimental data of References 19 and 26, which show a reduction of microscale λ near TDC with an increase in compression ratio. Also, the variations of l^* are in accord with the recent direct length scale measurements of Reference 27 in a disc-chamber engine for the period θ = 320°–380° CA.

During expansion (θ = 360°–450° CA), l^* rapidly increases initially due to the influence of expansion and the turbulence decay process, but thereafter tends towards an asymptote, whose level differs between the two models. τ^* increases rapidly in accord with the decay of u^*. The differences between the predictions of the two models are larger than during compression, with

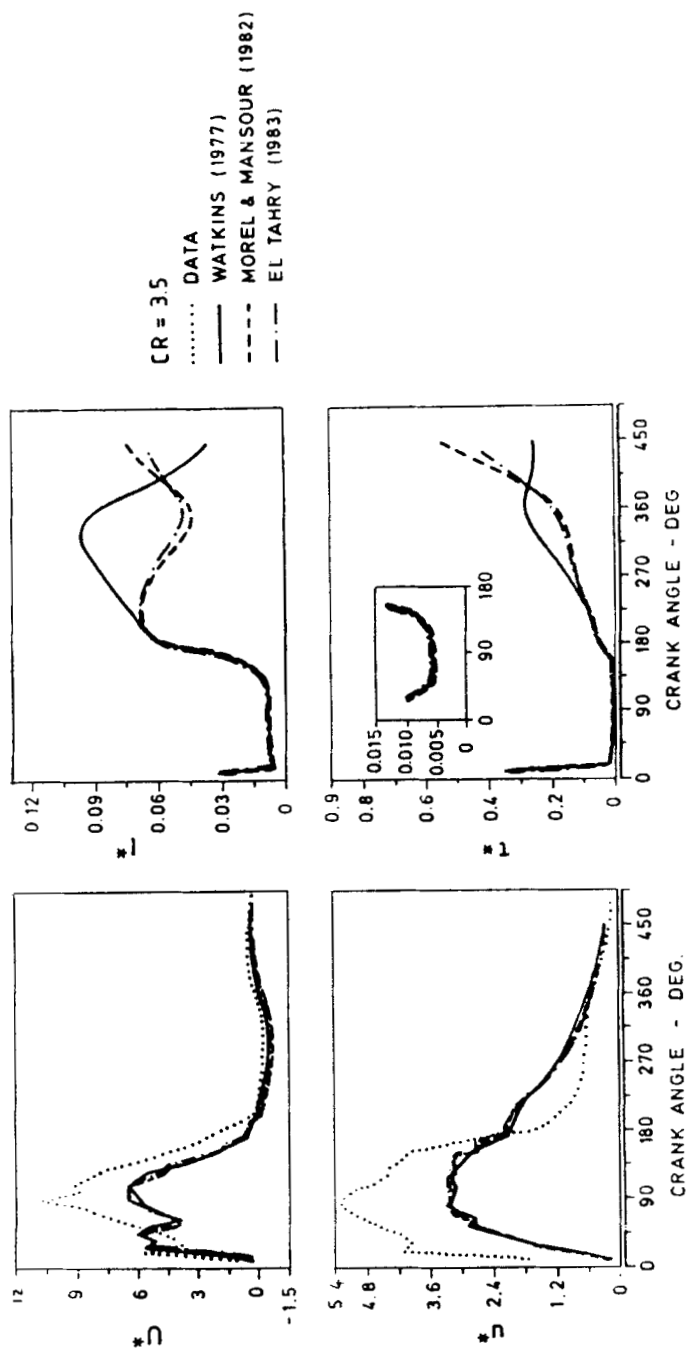

Figure 2. Measurements and predicted temporal variations of normalized flow parameters U^*, u^*, l^* and τ^* at monitoring location for case I

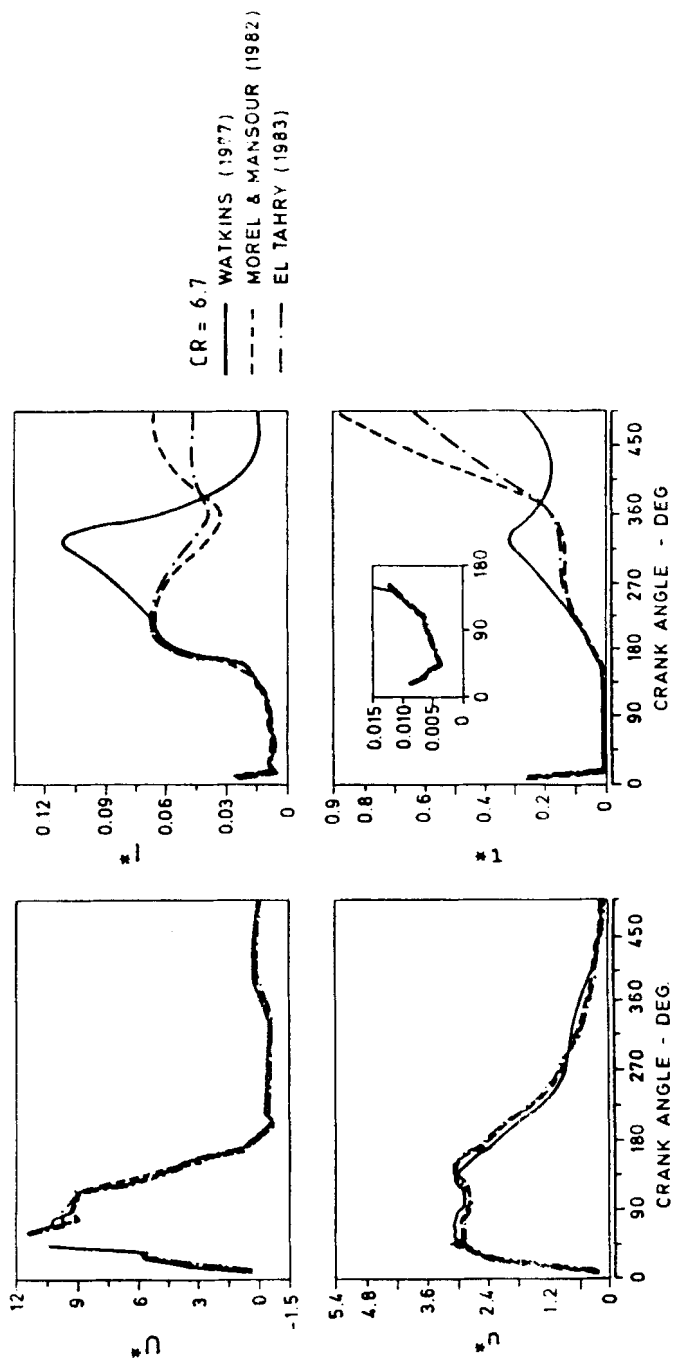

Figure 3. Predicted temporal variations of normalized flow parameters U^*, u^*, l^* and τ^* at monitoring location for case II

the MM version producing the largest increases of l^* and τ^*. This departure of the predictions is due to the increased significance of the compressibility term in the ε-equation as a consequence of rapid increase of τ^*, for as noted earlier its production and destruction terms have a τ^{-1} multiplier.

It appears from the above evidence that on the basis of consistency and compatibility of variations of the turbulence parameters, either the Morel and Mansour[2] or El Tahry[3] variant could be chosen. On physical grounds, the variation of l^* during expansion given by the Morel and Mansour[2] model appears more plausible, for it may be expected that under the influences of the turbulence decay and expansion, l should grow to levels similar to that attained at early compression, since the only constraint on the growth of l is then the engine bore. However, it must be pointed out that due to the rapid increase of τ during expansion (Figures 2(d) and 3(d)), the instantaneous time scale ratio $\tau\nabla\cdot\mathbf{U}$ may become large enough for the flow to be in a state of rapid distortion. The study of Wu *et al.*[7] indicates that under these conditions neither model is able to predict the correct turbulence behaviour.

CONCLUSIONS

(i) The extent of influence of compressibility effects on turbulence strongly depends on the dissipation time scale τ, which is determined by the induction history. Therefore those studies that employ arbitrary, non-representative τ in their analysis of compression effects may produce misleading results.

(ii) The ratio of the dissipation time scale to the time scale of compression at the start of the compression stroke in engines is small ($\tau^* = 0{\cdot}1$–$0{\cdot}2$) and independent of engine speed. Thus the compression process is slow and rapid distortion theory is inapplicable. The conditions of the latter may however apply during expansion, owing to the rapid increase of the dissipation time scale that occurs at this time.

(iii) The influence of the compressibility terms in the ε-equation is, for the range of multiplying coefficient values contained in the different turbulent model variants, marginal for the levels of τ attained during compression. Significant effects are however observed during expansion.

(iv) The Morel and Mansour[2] and El Tahry[3] models are both suitable for application to engine flows, but the Watkins[1] model is unsuitable.

ACKNOWLEDGEMENT

This work was performed at Imperial College of Science and Technology, London.

APPENDIX I

The relations for C_1' and C_1'' for a general compression strain field are[2]

$$C_1' = C_1 + a\,(C_1 - 1{\cdot}5),$$

$$C_1'' = 3 + 3/2n,$$

in which $C_1 = 1{\cdot}44$ and 'a' and 'n' are functions of the strain rate tensor of the form

$$a = 3(S_{11}^2 + S_{22}^2 + S_{33}^2)/(|S_{11}| + |S_{22}| + |S_{33}|)^2 - 1{\cdot}0,$$

$$n = 3 - \sqrt{(2a)}.$$

APPENDIX II

The compressibility term due to El Tahry[3] (note that $C_4 = 1$) can be expressed as

$$C_4 \frac{\rho\varepsilon}{\mu}\frac{\mathrm{d}\mu}{\mathrm{d}t} = C_4\,\rho\varepsilon\frac{\mathrm{d}}{\mathrm{d}t}\ln\mu. \tag{11}$$

Substituting for μ-dependence on temperature T, according to Sutherland's law, gives

$$C_4\,\rho\varepsilon\frac{\mathrm{d}}{\mathrm{d}t}\left(\ln\frac{1{\cdot}458\times10^{-6}\,T^{1{\cdot}5}}{T+110{\cdot}4}\right), \tag{12}$$

which after manipulation yields

$$C_4\,\rho\varepsilon\left(1{\cdot}5-\frac{T}{T+110{\cdot}4}\right)\frac{\mathrm{d}}{\mathrm{d}t}\ln T. \tag{13}$$

Assuming a polytropic compression,

$$Pv^n = \text{const.} \tag{14}$$

The temperature variation can be expressed as

$$T = \frac{\text{const.}}{R}\rho^{n-1}, \tag{15}$$

where R is the gas constant.

Substitution of relation (15) in (13) renders the compressibility term as

$$C_4(n-1)\,\rho\varepsilon\left(1{\cdot}5-\frac{T}{T+110{\cdot}4}\right)\frac{1}{\rho}\frac{\mathrm{d}\rho}{\mathrm{d}t}. \tag{16}$$

Invoking the continuity and neglecting the spatial variations of density renders

$$\frac{1}{\rho}\frac{\mathrm{d}\rho}{\mathrm{d}t} = -\nabla\cdot\mathbf{U}. \tag{17}$$

Substitution of relation (17) in (16) gives

$$C_4(n-1)\left(1{\cdot}5-\frac{T}{T+110{\cdot}4}\right)\rho\varepsilon\nabla\cdot\mathbf{U}. \tag{18}$$

For a polytropic compression $n \simeq 1{\cdot}3$ and the range of temperature variations typical of the compression/expansion stroke ($T = 300$–1000 K),

$$-C_4(n-1)\left(1{\cdot}5-\frac{T}{T+110{\cdot}4}\right) \simeq -0{\cdot}23 \text{ to } -0{\cdot}18.$$

REFERENCES

1. A. P. Watkins, 'Flow and heat transfer in piston/cylinder assemblies', *Ph.D. Thesis*, University of London, 1977.
2. T. Morel and N. N. Mansour, 'Modelling of turbulence in internal combustion engines', *SAE Paper 820040*, 1982.
3. S. H. El Tahry, 'k–ε equation for compressible reciprocating engine flows', *AIAA J. Energy*, **7**, 345–353 (1983).
4. J. I. Ramos and W. H. Sirigano, 'Axisymmetric flow model in a piston–cylinder arrangement with detailed analysis of the valve region', *SAE Paper 800286*, 1980.
5. F. Grasso and F. V. Bracco, 'Computed and measured turbulence in axisymmetric reciprocating engines', *AIAA J.*, **21**, 601–607 (1983).

6. W. C. Reynolds, 'Modelling of fluid motions in engines—an introductory overview', in J. N. Mattavi and C. A. Amann (eds), *Combustion Modelling in Reciprocating Engines*, Plenum Press, 1980, pp. 41–65.
7. C. T. Wu, J. H. Ferziger and D. R. Chapman, 'Simulation and modelling of homogeneous compressed turbulence', Department of Mechanical Engineering, Stanford University, 1985.
8. B. Ahmadi-Befrui, C. Arcoumanis, A. F. Bicen, A. D. Gosman, A. Jahanbakhsh and J. H. Whitelaw, 'Calculation and measurements of the flow in a motored model engine and implication for open-chamber, direct-injection engines', in S. Carmai *et al.* (eds), *Three Dimensional Turbulent Shear Flows*, ASME, 1982, pp. 1–9.
9. B. Ahmadi-Befrui, A. D. Gosman and A. P. Watkins, 'Prediction of in-cylinder flow and turbulence with three versions of k-ε turbulence model and comparison with data', in T. Uzkan (ed.), *Flows in Internal Combustion Engines—II*, ASME, 1984, pp. 27–38.
10. B. Ahmadi-Befrui, 'Analysis of flow evolution in the cylinders of motored reciprocating engines', *Ph.D. Thesis*, University of London, 1985.
11. A. D. Gosman, R. J. R. Johns and A. P. Watkins, 'Development of prediction methods for in-cylinder processes in reciprocating engines', in J. N. Mattavi and C. A. Amann (eds), *Combustion Modelling in Reciprocating Engines*, Plenum Press, 1980, pp. 69–124.
12. R. W. Bilger, 'A note on Favre averaging in variable density flows', *Combust. Sci. Technol.*, **11**, 215–217 (1975).
13. W. P. Jones, 'Models for turbulent flows with variable density and combustion', *Von Karman Institute for Fluid Dynamics Lecture Series 1979–2*, 1979.
14. F. H. Harlow and P. I. Nakayama, 'Transport of turbulence energy decay rate', *Los Alamos Sci. Lab. Report LA-3854*, 1968.
15. K. C. Muck and A. J. Smits, 'The behaviour of compressible boundary layer under incipient separation conditions', *Proc. 4th Symp. on Turbulent Shear Flows*, 1983, pp. 2·15–2·20.
16. R. Narashima and P. R. Viswanath, 'Reverse transition at an expansion corner in supersonic flow', *AIAA J.*, **13**, 693 (1975).
17. P. Bradshaw, 'Review—complex turbulent flows', *Trans. ASME*, 146–154, June (1975).
18. B. E. Launder and D. B. Spalding, *Lectures in Mathematical Models of Turbulence*, Academic Press, London, 1972.
19. D. R. Lancaster, 'Effects of engine variables on turbulence in a spark-ignition engine', *SAE Paper 760159*, 1976.
20. P. O. Witze, 'Measurements of the spatial distribution and engine speed dependence of turbulent air motion in an IC engine', *SAE Paper 770220*, 1977.
21. R. J. Tabaczynski, 'Turbulence and turbulent combustion in spark-ignition engines', in N. A. Chigier (ed.), *Progress in Energy and Combustion Science, Student Edition 1*, Pergamon Press, 1979.
22. G. K. Batchelor, *The Theory of Homogeneous Turbulence*, Cambridge University Press, 1960.
23. A. G. Prudnikov, 'Some measurements of the turbulence of air flows in industrial tubes', *NASA Tech. Trans. F-97*, 1963, pp. 85–96.
24. M. Tsuge, H. Kido, K. Kato and Y. Nomiyama, 'Decay of turbulence in a closed vessel (2nd Report, Time-scales of turbulence)', *JSME*, **17**, 587–594 (1974).
25. A. A. Townsend, *'The Structure of Turbulent Shear Flows*, 1st Edn, Cambridge University Press, 1956.
26. J. C. Dent and N. S. Salama, 'The measurement of the turbulence characteristics in an internal combustion engine cylinder', *SAE Paper 750886*, 1975.
27. R. A. Fraser, P. G. Felton, F. V. Bracco and D. A. Santavicca, 'Preliminary turbulence length scale measurements in a motored IC engine', *SAE Paper 860021*, 1986.